

# Propagation of the $1\mu\text{m}$ High-Power Beam from a Solid-State Heat-Capacity Laser

*C.B. Dane, J.R. Morris, A.M. Rubenchik, and C.D. Boley*

**June 25, 2002**

**U.S. Department of Energy**

Lawrence  
Livermore  
National  
Laboratory

## DISCLAIMER

This document was prepared as an account of work sponsored by an agency of the United States Government. Neither the United States Government nor the University of California nor any of their employees, makes any warranty, express or implied, or assumes any legal liability or responsibility for the accuracy, completeness, or usefulness of any information, apparatus, product, or process disclosed, or represents that its use would not infringe privately owned rights. Reference herein to any specific commercial product, process, or service by trade name, trademark, manufacturer, or otherwise, does not necessarily constitute or imply its endorsement, recommendation, or favoring by the United States Government or the University of California. The views and opinions of authors expressed herein do not necessarily state or reflect those of the United States Government or the University of California, and shall not be used for advertising or product endorsement purposes.

This work was performed under the auspices of the U. S. Department of Energy by the University of California, Lawrence Livermore National Laboratory under Contract No. W-7405-Eng-48.

This report has been reproduced directly from the best available copy.

Available electronically at <http://www.doc.gov/bridge>

Available for a processing fee to U.S. Department of Energy  
And its contractors in paper from  
U.S. Department of Energy  
Office of Scientific and Technical Information  
P.O. Box 62  
Oak Ridge, TN 37831-0062  
Telephone: (865) 576-8401  
Facsimile: (865) 576-5728  
E-mail: [reports@adonis.osti.gov](mailto:reports@adonis.osti.gov)

Available for the sale to the public from  
U.S. Department of Commerce  
National Technical Information Service  
5285 Port Royal Road  
Springfield, VA 22161  
Telephone: (800) 553-6847  
Facsimile: (703) 605-6900  
E-mail: [orders@ntis.fedworld.gov](mailto:orders@ntis.fedworld.gov)  
Online ordering: <http://www.ntis.gov/ordering.htm>

OR

Lawrence Livermore National Laboratory  
Technical Information Department's Digital Library  
<http://www.llnl.gov/tid/Library.html>

# **Propagation of the 1 $\mu$ m high-power beam from a solid-state heat-capacity laser**

C. Brent Dane, James R. Morris, Alexander M. Rubenchik, and Charles D. Boley  
Lawrence Livermore National Laboratory

June 25, 2002

Executive Summary .....	1
Introduction and purpose.....	2
Wavelength .....	2
Optical diffraction and beam director diameter.....	3
Atmospheric absorption and thermal blooming .....	4
Atmospheric scattering.....	7
Atmospheric turbulence.....	8
Numerical modeling of power delivery to target .....	9
Solid-state laser pulsed format.....	10
Summary.....	13

## **Executive Summary**

The propagation of a high average power laser beam through the atmosphere is affected by optical diffraction, atmospheric absorption, scattering, turbulence, and thermal blooming. Each of these effects depends on the optical wavelength of the laser beam. The results of preliminary analyses suggest that a 100kW solid-state laser could share the effectiveness of a deuterium fluoride chemical laser having 2-3X the average output power, providing very favorable projections for the utility of a 100kW mobile SSHCL.

## Introduction and purpose

A solid-state laser system, used as a directed energy defensive weapon, possesses many compelling logistical advantages over high-average-power chemical laser systems. As an electrically-powered laser, it uses no chemicals, generates no effluents, and requires no specialized logistics support — the laser is recharged by running the vehicle engine. It provides stealth, having low signature operation without the generation of temperature, smoke, or visible light. It is silent in operation, limited only by the onboard vehicle electrical charging and propulsion system. Using the heat-capacity mode of operation, scaling of average power from a solid-state laser has been demonstrated beyond 10kW and work in progress will result in the demonstration of a 100kW solid-state heat-capacity laser (SSHCL). The heat-capacity approach provides unprecedented power-to-weight ratios in a compact platform that is readily adapted to mobile operation. A conceptual engineering and packaging study has resulted in a 100kW SSHCL design that we believe can be integrated onto a hybrid-electric HMMWV or onto new vehicle designs emerging from the future combat system (FCS) development. 100kW has been proposed as a power level that demonstrates a significant scaling beyond what has been demonstrated for a solid-state laser system and which could have a significant lethality against target sets of interest. However, the characteristics of heat-capacity laser scaling are such that designs with output powers in excess of 1MW can be readily formulated.

An important question when addressing the military utility of a high-power solid-state laser system is that of the required average power during engagement with a target. The answer to this question is complex, involving atmospheric propagation, beam interaction with the target, and the damage response of the target. Successful target shoot-downs with the THEL deuterium fluoride (DF) laser system provide what is probably the best understanding of power requirements for a directed energy weapon against many threats of interest. In this paper, we discuss the pertinent parameters that affect the propagation of a high average power laser beam to target and examine how these parameters compare at the 1.06 and 3.8 $\mu$ m wavelengths of the SSHCL and DF laser systems. The result of the analysis presented here suggests that a 100kW solid-state laser could share the effectiveness of a DF laser having 2-3X the average output power, providing very favorable projections for the utility of a 100kW mobile SSHCL.

## Wavelength

A high average power, pulsed solid-state laser system is based on the 1 $\mu$ m lasing transition in the neodymium (Nd) or ytterbium (Yb) ion doped in a solid-state, crystalline host. The solid-state laser's 1 $\mu$ m output wavelength falls in the near-infrared portion of

the electro-magnetic spectrum and is invisible to the human eye. This wavelength is approximately one-fourth that of the DF chemical laser mid-infrared wavelength of 3.8 $\mu$ m resulting in a number of characteristics that are distinctly different from a DF chemical laser. The wavelength of a laser system is a critical parameter that affects the amount of divergence imposed by optical diffraction, the way the beam responds to turbulence-induced distortions in the atmosphere, and the power losses due to molecular and aerosol absorption, aerosol scattering, and thermally-induced blooming. In some cases, the 1 $\mu$ m wavelength has significant advantages such as for decreased diffraction and decreased molecular absorption. Atmospheric absorption is the dominant contributor to increased beam divergence by thermal blooming. Absorption of the beam by carbonaceous aerosols (smoke, urban pollution) can be more pronounced at the 1 $\mu$ m wavelength. There are only small differences between the effect of atmospheric turbulence on the propagation of laser beams for the solid-state and DF wavelengths, slightly favoring 3.8 $\mu$ m. However, a large portion of the distortions introduced by turbulence are readily correctable using adaptive optical beam director systems.

### **Optical diffraction and beam director diameter**

Due to the wave nature of light, a certain minimum divergence is imposed on a laser beam by optical diffraction for a given beam diameter. This minimum divergence is often referred to as the diffraction-limit and is directly proportional to the wavelength. The maximum irradiance (W/cm<sup>2</sup>) that can be placed on an object at the beam's focus is inversely proportional to the square of the beam divergence. For this reason, given beams of the same diameter and same power, the theoretical maximum irradiance that can be placed on a target using a beam from a solid-state laser at 1 $\mu$ m is 13X higher than that for wavelength of 3.8 $\mu$ m. It is important to recognize, however, that there are a number of factors that could increase the divergence of the laser beam to a value greater than the diffraction limit including atmospheric turbulence, thermal blooming, and uncompensated distortions within the laser and the beam director. The distortion imposed by atmospheric turbulence and distortions in the optics of the beam director can be corrected using linear adaptive optics such as deformable mirrors. Thermal blooming, however, must be minimized since the increased divergence imposed by this nonlinear effect is not readily correctable. Since the diffraction-limited divergence depends on the beam size, the effect of diffraction for the DF 3.8 $\mu$ m wavelength could be made equal to that for 1 $\mu$ m by using a beam director that is approximately 3.6X the diameter of that used for a solid-state laser. However, the cubic scaling of mass and volume as well as the need for high pointing and tracking agility make this a very unattractive solution. The following table is a simple illustration of the effect of wavelength on the maximum theoretically attainable irradiance on target at a distance of

5km using a laser system with an average power of 200kW and a beam diameter of 30cm.

<i>Target parameters</i>	<i>3.8<math>\mu</math>m (DF)</i>	<i>1.3<math>\mu</math>m (COIL)</i>	<i>1.06<math>\mu</math>m (SS)</i>
<i>Spot size</i>	7.6cm	2.6cm	2.1cm
<i>Spot area</i>	45.4cm <sup>2</sup>	5.3cm <sup>2</sup>	3.5cm <sup>2</sup>
<i>Irradiance</i>	4.4kW/cm <sup>2</sup>	37.7kW/cm <sup>2</sup>	56.6kW/cm <sup>2</sup>

**Table I** – Theoretical maximum delivered irradiance at 5km using a 200kW laser and a 30cm beam director.

### Atmospheric absorption and thermal blooming

As a laser beam propagates to its intended target, a portion of its power is absorbed by the intervening atmosphere. There are two important effects of this absorption. The first is that the power in the beam is reduced, lowering the irradiance (W/cm<sup>2</sup>) that can be delivered to the target. Of generally more significance, however, is that the absorption by the atmosphere causes heating. The resulting thermal gradients in the path of the beam introduce optical distortions, increasing the effective divergence and further lowering the irradiance on target. This process is referred to as thermal blooming. The beam break-up due to thermal blooming has a nonlinear dependence on the irradiance distribution within the laser beam and propagation distance. This nonlinearity prevents an effective method of pre-compensation at the beam director source. Since there is a time scale associated with the atmospheric heating that leads to blooming, the impact of this phenomenon is sensitive to atmospheric motion relative to the laser beam. This can take the form of naturally occurring wind or pseudo-wind resulting from the slewing of the laser beam through the air as it tracks a target. For example, in the absence of wind, strong thermal blooming could make a nose-on target engagement very difficult while a side-on engagement of a high-speed target could reduce thermal blooming.

There are two sources of atmospheric absorption that can lead to thermal blooming: molecular absorption and aerosol absorption.

*Molecular absorption* - Molecular absorption is the result of spectroscopic transitions in the gaseous components of the atmosphere. The solid-state laser wavelength of 1 $\mu$ m has a tremendous advantage with regard to molecular absorption. While the absorption of the 3.8 $\mu$ m DF laser wavelength at sea level is typically 5-6%/km, absorption at 1 $\mu$ m is for all practical purposes negligible. Note that, without even considering the effects of thermal blooming, an absorptive attenuation of 5%/km results in a 40% power loss over

a 10km propagation distance through the atmosphere. The following figure shows high resolution spectra illustrating the very low molecular absorption for solid-state laser wavelengths of 1.064 (Nd:YAG), 1.061 (Nd:GGG), and 1.053 (Nd:glass). In all cases, the absorption coefficient is less than 0.01%/km for solid-state.

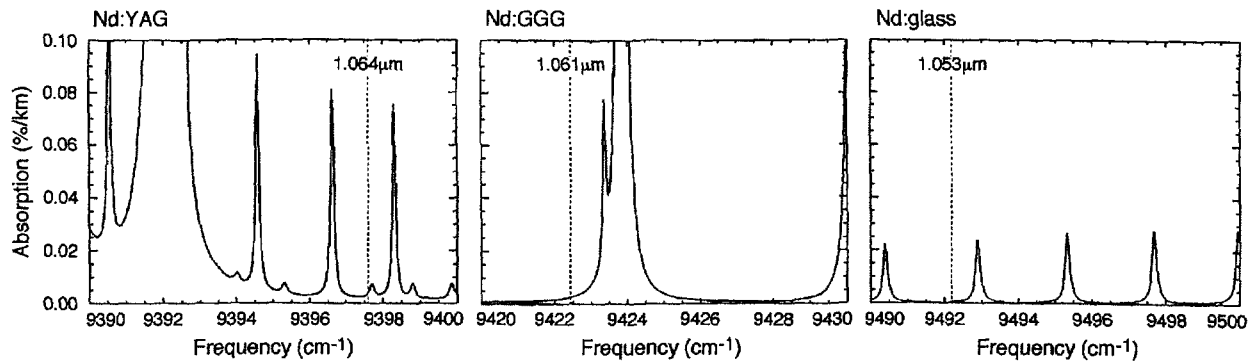


**Figure 1** – High resolution atmospheric absorption spectra for Nd laser transition wavelengths in several relevant solid-state hosts. Note that the vertical scale is in %/km.

**Aerosol absorption** - The second source of atmospheric absorption is from aerosols. These are small particles of liquid or solid material finely dispersed through the air. Examples of these aerosols are dust and fog. Since aerosols are not gaseous constituents of the atmosphere, their composition and concentration is highly variable with respect to weather, location, altitude, and the local terrain. To illustrate typical magnitudes of aerosol absorption, LOWTRAN7 was used with its rural boundary layer model<sup>1</sup> for the 0-2km altitude region. Above 2km in altitude, the tropospheric aerosol model was used. The following aerosol absorption coefficients are predicted.

Altitude (km)	3.8 $\mu$ m (DF) %/km	1.3 $\mu$ m (COIL) %/km	1.06 $\mu$ m (SS) %/km
0.0	0.2	0.7	0.7
1.0	0.1	0.5	0.5
2.0	0.1	0.3	0.3
3.0	0.0	0.1	0.1
4.0	0.0	0.1	0.1
5.0	0.0	0.0	0.0

**Table II** – Atmospheric aerosol absorption coefficients for rural conditions and 23km visibility.

Altitude (km)	3.8 $\mu$ m (DF) %/km	1.3 $\mu$ m (COIL) %/km	1.06 $\mu$ m (SS) %/km
0.0	0.4	1.6	1.8
1.0	0.4	1.9	2.0
2.0	0.1	0.3	0.3
3.0	0.0	0.1	0.1
4.0	0.0	0.1	0.1
5.0	0.0	0.0	0.0

**Table III** – Atmospheric aerosol absorption coefficients for rural conditions and 10km visibility.

Based on molecular absorption alone, the conclusion might be made that the solid-state laser beam is not subject to thermal blooming. Although molecular absorption is negligible for the 1 $\mu$ m wavelength, the absorption coefficients presented in these charts illustrate that aerosol absorption at 1 $\mu$ m is not. Under 10km visibility conditions, aerosol absorption at 1 $\mu$ m reaches 2%/km compared to the aerosol absorption of 0.4%/km and molecular absorption of 5-6%/km for the DF laser at 3.8 $\mu$ m. Note that there is a strong altitude dependence of the aerosol absorption at both wavelengths which will accentuate its effects for lower altitude target engagements.

The discussion of aerosol absorption is not complete before considering carbonaceous aerosols present in smoke or smog. These exhibit stronger absorption at 1 $\mu$ m than at 3.8 $\mu$ m. In the following chart, absorption coefficients are compared for these two wavelengths under urban carbonaceous aerosol conditions for both 23 and 10km visibility.

Visibility (km)	3.8 $\mu$ m (DF) %/km	1.06 $\mu$ m (SS) %/km
23	0.9	2.3
10	2.7	6.7

**Table IV** – Atmospheric aerosol absorption coefficients for urban carbonaceous aerosols for 23 and 10km visibilities.

For carbonaceous aerosols, the absorption coefficient at 1 $\mu$ m for 23km visibility is increased to approximately the same value (2%/km) for 10km visibility conditions in the presence of rural aerosols. Note that, although the absorption coefficient for carbonaceous aerosols at 10km visibility is quite large at 1 $\mu$ m, it is still less than the overall atmospheric absorption for 3.8 $\mu$ m when the contributions of both molecular and aerosol absorption are considered. For visibilities less than 10km in the presence of smoke, the propagation of both wavelengths will be significantly degraded by thermal blooming.

## Atmospheric scattering

Scattering is a term generally used to describe the resulting optical diffraction when a light wave interacts with small particles (an aerosol) that are irregularly arranged in the path of the beam. There are two sources of beam extinction when the laser beam passes through an aerosol: absorption, as discussed in the previous section, and scattering. Optical scattering is the result of diffraction around the particles and spreads some part of the incident laser beam into a large cone of angles while leaving the divergence of the primary beam largely intact. It is important to note that, unlike optical absorption in aerosols, optical scattering does not deposit heat into the air and therefore does not contribute to thermal blooming. However, scattering does have a measurable effect on the attenuation of the laser beam by the atmosphere and affects the ability to deliver power to an intended target.

Rayleigh scattering describes the limit of optical scattering in which the particles are very small in comparison to the optical wavelength, such as the molecules making up the gaseous atmosphere. In this case, the magnitude of scattering losses increases as  $\lambda^{-4}$ . However, this scaling is not appropriate to the discussion here since Rayleigh scattering losses are insignificant at the 1 $\mu$ m and 3.8 $\mu$ m wavelengths of the solid-state and DF laser systems. The particle size for the atmospheric aerosols of concern for scattering loss with these laser systems is comparable to the optical wavelength and a  $\lambda^{-1}$  scaling in the magnitude of scattering losses is observed. As seen from the LOWTRAN7 predictions presented below, this increases the scattering losses by ~3.5X for the solid-state wavelength. Again, note that this is an issue of linear loss of power from the laser since scattering losses do not generate the nonlinear losses associated with optical absorption and thermal blooming.

Using the same LOWTRAN7 aerosol model previously described for aerosol absorption, optical scattering can be predicted as a function of altitude. The data is presented for 23km and 10km visibility conditions.

Altitude (km)	3.8 $\mu$ m (DF) %/km	1.3 $\mu$ m (COIL) %/km	1.06 $\mu$ m (SS) %/km
0.0	1.6	4.6	6.0
1.0	0.9	2.7	3.6
2.0	0.5	1.7	2.3
3.0	0.0	0.9	1.1
4.0	0.0	0.4	0.6
5.0	0.0	0.2	0.3

**Table IV** – Atmospheric aerosol scattering extinction coefficients for rural conditions and 23km visibility.

<i>Altitude (km)</i>	<i>3.8<math>\mu</math>m (DF) %/km</i>	<i>1.3<math>\mu</math>m (COIL) %/km</i>	<i>1.06<math>\mu</math>m (SS) %/km</i>
0.0	3.8	10.9	14.4
1.0	3.5	10.5	13.9
2.0	0.6	1.7	2.3
3.0	0.0	0.8	1.1
4.0	0.0	0.4	0.6
5.0	0.0	0.2	0.3

**Table V** – Atmospheric aerosol scattering extinction coefficients for rural conditions and 10km visibility.

Just as for the case of aerosol absorption, estimates can also be made for aerosol scattering by carbonaceous aerosols found in smoke and smog under different visibility conditions.

<i>Visibility (km)</i>	<i>3.8<math>\mu</math>m (DF) %/km</i>	<i>1.06<math>\mu</math>m (SS) %/km</i>
23	2.2	7.3
10	5.3	18.0

**Table VI** – Atmospheric scattering extinction coefficients for urban carbonaceous aerosols for 23 and 10km visibilities.

### Atmospheric turbulence

As a laser beam propagates through the atmosphere, it is distorted by turbulence in the air. The aberrations are primarily caused by variations in the refractive index resulting from fluctuations in temperature within the beam path. These fluctuations arise from the convective mixing of air of different temperatures and the resulting turbulence causes both pointing error and increased divergence as the beam propagates toward the intended target. Since the velocity of the air motion that generates this turbulence is much smaller than the speed of sound, the air can be treated as an incompressible ideal liquid and the distribution of the atmospheric aberrations is well described by a scaling function called the Kolmogorov law<sup>2</sup>. Under conditions that the turbulence-induced beam divergence dominates the diffraction-limited divergence (see previous discussion of the diffraction-limit), then it is often useful to introduce the concept of the Fried's coherence diameter<sup>3</sup>, generally referred to as  $r_0$ . In this case, the time-averaged focal spot diameter on target is one that would be consistent with that a diffraction-limited beam propagating from an aperture of size  $r_0$ . As magnitude of the turbulence increases, the coherence diameter  $r_0$  decreases, proportionally increasing the spot diameter on target. Using the Kolmogorov scaling of the spatial scaling of turbulence-induced distortions, it can be shown that  $r_0$  scales as  $\lambda^{1.2}$  where  $\lambda$  is the laser wavelength. Since the divergence of the time averaged beam is proportional to  $\lambda/r_0$ , the time-averaged divergence of the laser beam and resulting spot size on target then

scales as  $\lambda^{-0.2}$ . This suggests that the divergence of a 1 $\mu$ m solid-state laser beam would be 1.3X that for a 3.8 $\mu$ m DF laser beam under the same atmospheric turbulence conditions.

It is important to recognize that turbulence-induced distortion of the laser beam is a linear process that can be corrected by existing, well-developed adaptive optical technology. Although for a given beam director diameter, the uncorrected turbulence-distorted spot size on target of a 1 $\mu$ m laser is expected to be 1.3X larger than that of a 3.8 $\mu$ m laser, the corrected spot size on target could potentially be 3.6X smaller than for 3.8 $\mu$ m. Decreased optical diffraction at the shorter solid-state wavelength provides very high leverage for adaptive optical correction techniques.

### **Numerical modeling of power delivery to target**

In this paper, a number of factors affecting the relative propagation of 3.8 and 1 $\mu$ m high power laser beams have been presented and discussed. Diffraction, absorption, thermal blooming, and small-scale scattering all contribute to the delivery of power to a distant target and must be included in attempts to predict relative performance at each wavelength.

A simulation was conducted using mid-latitude summer molecular absorption. Thermal blooming was treated as per H. Breaux, *et al.*<sup>4</sup> assuming CW beams and the  $C_N^2$  model of atmospheric turbulence from the I.R. Handbook was used.<sup>5</sup> Rural aerosols for 23km visibility were used with an exponential fall-off in concentration with an altitude constant of 3.5km. The laser beam at both wavelengths was set to an average power of 200kW and a diameter at the beam director of 30cm. Both beams were assumed to have an effective divergence of 2X the diffraction-limit at the launch point although, since no adaptive correction of the atmosphere was used in the simulation, the divergence characteristics of the propagation is dominated by turbulence-induced distortions. A wind speed of 2.5m/s was used and the simulation was repeated for angular slew rates of 5 and 50mrad/s to illustrate the contributions from thermal blooming. Constant irradiance contours were calculated as a function of ground range and altitude for 5kW/cm<sup>2</sup> at the target. The parameters for this particular case are not intended to reflect specific laser system designs and are not optimized for either wavelength case, but were chosen as reasonable points for comparison.

Figure 2 depicts the result of this simulation at 1 and 3.8 $\mu$ m. As can be seen, a significantly enhanced (>3X) range is predicted at 1 $\mu$ m, for both angular slew rates. Note that this is a very significant result since the incident irradiance drops inversely proportional to the square of range. This suggests that, under these conditions, the average power from the solid-state laser could be reduced almost 10X to match the

irradiance on target at  $3.8\mu\text{m}$ . This  $1\mu\text{m}$  advantage would be lessened under more obscuring aerosol conditions but even at visibilities down to the 10km range, a 2-3X power ratio is expected. No correction for atmospheric turbulence was assumed in this simulation so that the advantage seen at  $1\mu\text{m}$  would be further increased by the use of adaptive optics in the beam director.

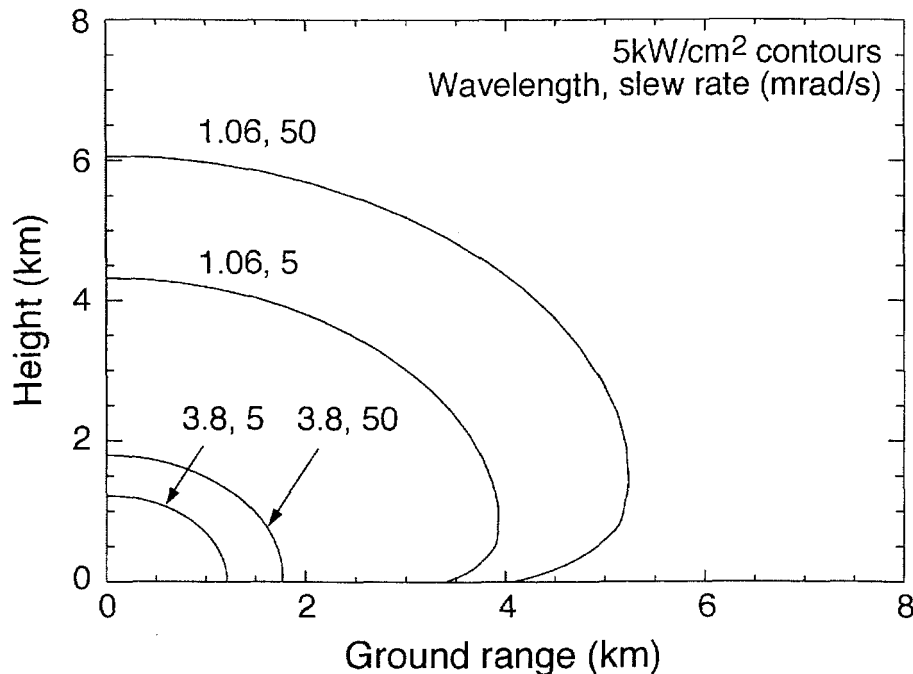


**Figure 2** – Propagation simulations for 30cm diameter beams with average power of 200kW. No atmospheric correction is assumed.

### Solid-state laser pulsed format

The solid-state heat-capacity laser (SSHCL) design generates its output as a train of pulses, rather than a continuous beam. A typical on-time duty-cycle is 10% meaning that during each laser pulse, the output power will be 10X the time-averaged power. For example, a 100kW heat-capacity laser will have a peak power, during each laser pulse, of 1MW. This pulsed format may have potential effects on the propagation of the beam to target as well as on the interaction of the beam with the surface of the target.

*Pulsed atmospheric propagation* – In the optical simulations that have been performed evaluating the effects of thermal blooming, the  $1\mu\text{m}$  laser beam has up until now been treated as CW, without a specific pulse format. Recently, we have begun to activate a time-resolved thermal blooming numerical code that should be able to evaluate the specific atmospheric response during individual laser pulses. Preliminary results suggest that pulse durations that are longer than the sound transit time across the on-

target beam diameter may have more thermal blooming than a CW laser of the same time-averaged power. Calculations indicate that these effects are most notable for long pulses ( $>1$ ms) and tightly focused beams (using adaptive optical correction) on the target that could be achieved at short range. In the most extreme conditions, where the beam width could be as small as 1-2cm at the target, the air heating corresponds to the power during the time the pulse is on rather than to the time-averaged power over a pulse-repetition period. However, an important consideration regarding thermal blooming at 1 $\mu$ m is related to the fact that atmospheric absorption at this wavelength is completely dominated by aerosol absorption. In this case, rather than a uniform, bulk absorption in the path of the beam that would result from molecular absorption, beam losses occur at discrete, sparsely distributed aerosol particles. Careful consideration of the timescales associated with the energy transfer from the heated aerosol and subsequent thermal conduction into the surrounding air is needed in order to accurately predict pulsed thermal blooming phenomena, an effect not presently accounted for in initial simulations. The granularity of aerosol absorption creates an effect called aureole scattering. The energy deposited in an aerosol particle is transferred to the surrounding air by thermal diffusion and creates a hot air bubble around the particle which can contribute to transient scattering losses. The granularity is expected to become unimportant when the bubble diameter grows to a few times a suitably weighted mean particle spacing, probably between 2 and 10ms. With an initial design of 500 $\mu$ s pulse duration, the SSHCL lies in an intermediate regime where there is both the possibility of overestimating thermal blooming and underestimating scattering losses.

These effects are under continuing study and have not been validated experimentally. The use of the 10kW (500J, 20Hz, 500 $\mu$ s) technology demonstration laser at HELSTF to conduct pulsed atmospheric propagation tests will be a critical step towards the optimization of the pulse energy, pulse duration, and pulse repetition frequency for a solid-state laser. The optimal laser design will of course depend on these issues of atmospheric propagation as well as the coupling of the high power beam with the target. The pulse duration and pulse repetition frequency flexibility provided by a solid-state laser will be key to this optimization.

*Pulsed target interaction* – While this is not strictly an atmospheric propagation issue, it is also an important consideration with regard to the optimal pulse format from a high average power SSHCL. We have demonstrated that the high peak power available from the pulsed output format opens up a new range of damage mechanisms, some of which exhibit rapid material removal from the surface of the target. However, even using conventional lethality mechanisms such as the rapid cook-off of high explosives by heating, there are distinct advantages to the high peak power of the pulsed format.

For spot sizes too large for significant material removal by several pulses (say  $\sim 4\text{cm}^2$ ), an SSHCL still deposits heat very effectively in a target. This follows from the fact that the metallic absorptivity increases with temperature, and during an SSHCL pulse, the surface temperature of a target rises sharply. In a metal, the absorption occurs practically at the surface. Once deposited, the heat conducts through the metal and when the interior temperature reaches a sufficient level, thermal damage mechanisms come into play. A CW laser, by contrast, cannot access the same high-temperature regime of the absorptivity. Therefore a given power level, a CW beam will result in less energy deposition and less damage potential.

To illustrate this advantage, consider a  $2\times 2\text{cm}^2$  spot on a 2mm thickness of steel. In the SSHCL case, it is exposed to 8 pulses at 200Hz with 100kW time-averaged power. In the CW case, it is exposed to this power continuously for the same amount of time (40ms). Figure 3 shows the calculated temperature of the front face versus time. In the SSHCL case, the temperature increases in a pulsed manner, reaching peaks about 1500C greater than in the CW case. The most critical information is conveyed in the right-hand plot, which shows the temperature at the rear face of the steel plate. The SSHCL has produced a temperature rise more than 100C greater than the CW laser in this very short engagement. Initial measurements using the 10kW flashlamp-pumped SSHCL presently in operation at HELSTF are consistent with this heating model.

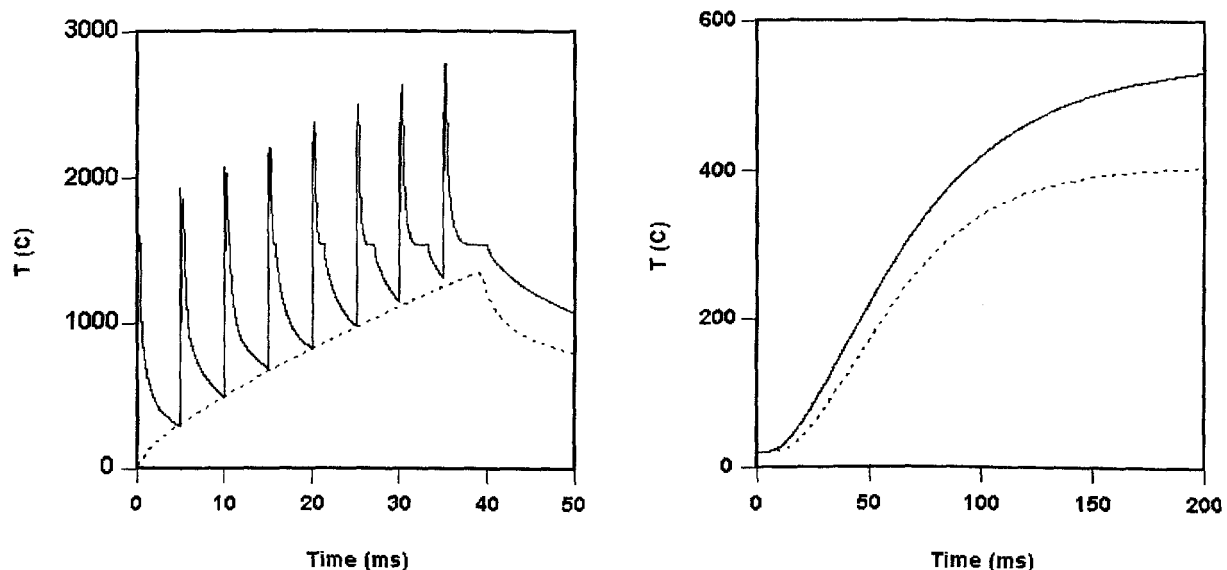


**Figure 3** – Simulated temperature rise at the front (left plot) and back (right plot) of a 2mm steel plate illuminated by a 100kW pulsed (solid line) and CW (dashed line) laser beam incident on a  $4\text{cm}^2$  spot.

It is important to point out that this illustration has omitted a feature favorable to the SSHCL case. This is the fact that the metallic absorptivity increases not only with temperature but also with laser frequency, providing an additional advantage over a CW

3.8 $\mu$ m laser beam. However, this increase with optical frequency is poorly quantified at elevated temperatures. For this reason, we used the same reflectivity vs. temperature response curve for both cases, thereby overestimating the CW temperature if it were actually being achieved with a 3.8 $\mu$ m beam.

## Summary

- For the same size beam director, 1 $\mu$ m provides a 13X higher maximum corrected irradiance (W/cm<sup>2</sup>) on target over 3.8 $\mu$ m.
- Typical molecular absorption (major contributor to thermal blooming) at 3.8 $\mu$ m is in the range of 5-6%/km compared to <<0.1%/km at 1 $\mu$ m. Thermal blooming is a nonlinear optical phenomenon, not readily corrected using adaptive optics.
- Aerosol absorption is higher at 1 $\mu$ m than at 3.8 $\mu$ m. However, at 10km visibility in rural aerosol conditions, the sum of molecular and aerosol absorption at 1 $\mu$ m is less than one-half that for 3.8 $\mu$ m.
- Absorption by carbonaceous aerosols offers the most significant propagation issue at the solid-state 1 $\mu$ m wavelength. 10km visibility in the presence of smog or smoke is the breakpoint at which the total atmospheric absorption for 1 $\mu$ m and 3.8 $\mu$ m is approximately equal. At shorter visibility ranges, 1 $\mu$ m absorption exceeds that at 3.8 $\mu$ m. However, strong absorption in low-visibility smoke-filled air will significantly degrade directed energy performance at both wavelengths.
- Atmospheric scattering due to aerosols typically scales as one over the wavelength ( $\lambda^{-1}$ ). However, small-scale scattering is a linear power loss mechanism that does not contribute to atmospheric heating and thermal blooming and therefore has less significant impact than absorption.
- The beam divergence due the contributions of atmospheric turbulence scales as  $\lambda^{-0.2}$ . However, these turbulence effects can be corrected using adaptive optical systems in the beam director. Decreased optical diffraction at 1 $\mu$ m provides large benefits for the use of these correction systems.
- The synthesis of the effects summarized here into a beam propagation model concludes that, under conditions of 23km visibility with rural aerosol composition, >3X increase in range for a fixed irradiance (W/cm<sup>2</sup>) on target is available at 1 $\mu$ m over that at 3.8 $\mu$ m. This suggests that the average power at 1 $\mu$ m could be decreased by almost 10X to match the irradiance on target at 3.8 $\mu$ m. Under more stressing aerosol

conditions, this factor could be reduced from 10X to 2-3X, still providing a significant advantage for the 1 $\mu$ m wavelength.

- Transient propagation effects could increase the thermal blooming for the solid-state pulsed output beam for engagements with very small spots on target (short-range penetration irradiance), requiring an optimization of the pulse duration and pulse repetition frequency. This potential effect is not completely characterized and needs further theoretical study and long-range propagation testing with the 10kW heat-capacity laser at HELSTF.
- The SSHCL pulsed output format provides improved coupling of the laser beam to a metal target, even under low irradiance conditions below vaporization thresholds. This experimentally validated effect is the result of the sharp rise in surface temperature and corresponding increase in metallic absorptivity during each laser pulse.

## Endnotes

1. F. X. Kneizys, *et al.*, AFGL-TR-80-0067, February 21, 1980.
2. A. N. Kolmogorov, "The Local Structure of Turbulence in Incompressible Viscous Fluid for Very Large Reynolds Numbers," *Doklady Akad. Nauk. USSR* **30**, 301 (1941).
3. D. L. Fried, "Statistics of a Geometric Representation of Wavefront Distortion," *Journal of the Optical Society of America* **55**, 1427-1435 (1965).
4. H. Breaux, W. Evers, R. Sepucha, and C. Whitney, "Algebraic model for CW thermal-blooming effects," *Appl. Opt.* **18**, 2638-2644 (1979).
5. R. E. Hufnagel, "Propagation through atmospheric turbulence," *The Infrared Handbook*, W. L. Wolfe and G. J. Zissis (eds.), Environmental Research Institute of Michigan, Michigan, 1989.